Multiple nonequilibrium steady states for one-dimensional heat flow

Fei Zhang,[1] Dennis J. Isbister,[1] and Denis J. Evans[2]

[1]*School of Physics, University of New South Wales, University College, ADFA, Canberra, ACT 2612, Australia*
[2]*Research School of Chemistry, Australian National University, Canberra, ACT 0200, Australia*

A nonequilibrium molecular dynamics model of heat flow in one-dimensional lattices is shown to have multiple steady states for any fixed heat field strength f_e ranging from zero to a certain positive value. We demonstrate that, depending on the initial conditions, there are at least two possibilities for the system's evolution: (i) formation of a stable traveling wave (soliton), and (ii) chaotic motion throughout the entire simulation. The percentage of the soliton-generating trajectories is zero for small field strength f_e, but increases sharply to unity over a critical region of the parameter f_e.

In recent years, the study of nonequilibrium statistical mechanics systems has attracted increasing attention. In particular, nonequilibrium molecular dynamics (NEMD) simulations of many-body systems have flourished [1–8]. In a NEMD system, an external (driving) force is coupled to the particle system and a thermostat then used to keep the system's temperature or total internal energy constant. The external force and the thermostat are usually modeled as deterministic modifications of the equations of motion; the thermostat removes (on average) excessive heat from the system. As a result, the NEMD system is typically deterministic, time reversible, and dissipative. In such a system the sum of all the Lyapunov exponents is negative, signifying the collapse of the comoving phase-space volume onto either a strange chaotic attractor or a limit cycle. In the long time limit, the NEMD system dynamics usually reaches a steady state and its trajectory eventually settles onto a fractal object in its associated phase space. In computer simulations and theoretical analysis [1–8] of NEMD systems it is very important to know *whether the NEMD steady state is unique* (especially for small fields) in the sense that all trajectories, no matter what the initial conditions are, settle onto the same attractor, be it chaotic or otherwise.

In this paper, we demonstrate that the steady state of a NEMD system can be *nonunique* even for vanishingly small fields. This is in sharp contrast to all previous numerical observations and theoretical assumptions. Using the Evans's NEMD heat flow algorithm [1,6] for the computation of the heat conductivity for a one-dimensional (1D) lattice of interacting particles [7,8], as an example, we show that for each applied field strength f_e ranging from 0 to f_{C2} (see following discussions) the system dynamics may either converge to a solitary wave (or loosely speaking, a soliton) within a finite time, or dwell on a low-dimensional chaotic attractor during the entire (long time) simulation. The final state depends on the initial conditions that are chosen randomly from the phase space. The probability of observing a soliton-state vanishes for small f_e, but exhibits a sharp transition from zero to unity over a critical parameter region of f_e. We show that the soliton corresponds to an exact solution for a traveling wave of the lattice, and that its shape, velocity, and amplitude can be determined from a differential-difference equation. These findings suggest that multiple nonequilibrium steady states should not be ignored in future computer simulations and theoretical studies of nonequilibrium systems.

We consider the NEMD equations of motion for heat flow in 1D lattices [1,6–8]:

$$\dot{q}_i = p_i/m,$$

$$\dot{p}_i = U'(q_{i+1}-q_i) - U'(q_i-q_{i-1}) + f_e D_i - \alpha p_i. \quad (1)$$

Here m is the ith particle's mass, q_i the displacement, and p_i the corresponding momentum; the function U represents the nearest-neighbor interparticle interaction potential; the $f_e D_i$ and αp_i terms model a heat field and a constant-energy thermostat, respectively, where

$$D_i = -\frac{1}{2}[U'(q_{i+1}-q_i) + U'(q_i-q_{i-1})]$$

$$+ \frac{1}{N}\sum_{j=1}^{N} U'(q_{j+1}-q_j), \quad (2)$$

and

$$\alpha = \frac{f_e}{2K}\sum_{i=1}^{N}\frac{p_i}{m}D_i, \quad K = \frac{1}{2}\sum_{i=1}^{N}\frac{p_i^2}{m}. \quad (3)$$

Note that the system's internal energy

$$\mathcal{H} = \sum_{i=1}^{N}\left[\frac{1}{2m}p_i^2 + U(q_{i+1}-q_i)\right] \quad (4)$$

is constant along a trajectory because from Eqs. (1)–(3) $d\mathcal{H}/dt \equiv 0$. This is in comparison with the constant-temperature thermostat used in previous studies [7,8]. Without the thermostat, the system's internal energy would increase gradually (for $f_e \neq 0$) and eventually cause numerical overflow in the computer simulations.

Like many other NEMD systems, system (1) is *deterministic* and *time reversible*. The time reversibility is inherited from the original Newtonian dynamics: at any point of a trajectory, if the signs of the velocities of all the particles are changed while their coordinates remain the same, then the particles, which move according to the dynamical system

(1), will trace back their positions exactly. For a mathematical definition of time reversibility, see Ref. [1], p. 183, Eq. (7.50).

The idea of the NEMD simulation is to calculate the thermal conductivity coefficient of the lattice by using the following formula:

$$\lambda = \lim_{f_e \to 0} \lim_{t \to \infty} \frac{\langle J_x(t) \rangle}{T f_e}, \tag{5}$$

where T is system's temperature, $J_x(t)$ is the heat flux,

$$J_x(t) = -\frac{1}{N} \sum_i \frac{p_i}{2m} [U'(q_{i+1} - q_i) + U'(q_i - q_{i-1})], \tag{6}$$

and the quantity $\langle J_x(t) \rangle$ in Eq. (5) is, in principle, a nonequilibrium *ensemble average*. As pointed out in the literature (e.g., [1]), this heat flow algorithm is valid in the weak field regime, i.e., $f_e \to 0$. In the strong field regime there is no known physical meaning or interpretation for the quantity, $\lim_{t \to \infty} \langle J_x(t) \rangle / (T f_e)$.

In many previous simulations [1,2,4–8] the nonequilibrium steady state was assumed to be unique (i.e., independent of the initial conditions), thus the ensemble average of $J_x(t)$ was replaced by a long time average. Moreover, in the fluctuation theorems of Evans and Searles [4] and the chaotic hypothesis of Gallavotti and Cohen [5], it is also assumed that the nonequilibrium steady state is generally unique and chaotic. However, in the following we will show that the present NEMD system can support at least two different types of steady states, the soliton and strange chaotic attractor, even for arbitrarily small external field f_e.

Soliton solutions

In order to show that Eq. (1) admits traveling wave or soliton solutions for any $f_e \geqslant 0$, we introduce a variable $Q_i = q_i - q_{i-1}$ and we set $m = 1$ without loss of generality. From Eq. (1) we can readily obtain

$$\ddot{Q}_i = U'(Q_{i+1}) - 2U'(Q_i) + U'(Q_{i-1}) - \frac{1}{2} f_e [U'(Q_{i+1})$$
$$- U'(Q_{i-1})] - \alpha \dot{Q}_i. \tag{7}$$

Taking into account the cyclic boundary conditions used for Eqs. (1), we find that the transformation $q_i - q_{i-1} = Q_i$, $i = 1, 2, \ldots, N$, has an inverse: $\mathbf{q}(t) = \mathbf{B} \cdot \mathbf{Q}(t)$, where $\mathbf{q}(t) = (q_1, q_2, \ldots, q_N)^T$ and $\mathbf{Q}(t) = (Q_1, Q_2, \ldots, Q_N)^T$ are column vectors, and $\mathbf{B}$ is an $N \times N$ matrix,

$$\mathbf{B} = \begin{bmatrix} 1 & \frac{1}{N} & \frac{2}{N} & \cdots & \frac{N-2}{N} & \frac{N-1}{N} \\ \frac{N-1}{N} & 1 & \frac{1}{N} & \cdots & \frac{N-3}{N} & \frac{N-2}{N} \\ \frac{N-2}{N} & \frac{N-1}{N} & 1 & \cdots & \frac{N-4}{N} & \frac{N-3}{N} \\ \vdots & \vdots & \vdots & \vdots & \vdots & \vdots \\ \frac{2}{N} & \frac{3}{N} & \frac{4}{N} & \cdots & 1 & \frac{1}{N} \\ \frac{1}{N} & \frac{2}{N} & \frac{3}{N} & \cdots & \frac{N-1}{N} & 1 \end{bmatrix}. \tag{8}$$

Substituting this into Eq. (3) we obtain

$$\alpha \equiv \alpha(\mathbf{Q}, \dot{\mathbf{Q}}) = -\frac{1}{2} f_e \frac{\dot{\mathbf{Q}}^T \mathbf{B}^T \cdot \mathbf{D}}{\dot{\mathbf{Q}}^T \mathbf{B}^T \mathbf{B} \dot{\mathbf{Q}}}, \tag{9}$$

where $\mathbf{D}$ is a column vector with $[U'(Q_{j+1}) + U'(Q_j)]$ being its jth element $(1 \leqslant j \leqslant N)$.

Equations (7) and (9) form a closed set of lattice dynamics equations for $\{Q_i(t), 1 \leqslant i \leqslant N\}$. Furthermore, we can seek solutions of the form $Q_i(t) = Q(i - Vt) \equiv Q(z)$ for traveling waves. Substituting this ansatz into Eq. (7) we obtain a nonlinear differential-difference equation,

$$V^2 Q''(z) = U'[Q(z+1)] - 2U'[Q(z)] + U'[Q(z-1)]$$
$$- \frac{1}{2} f_e [U'\{Q(z+1)\} - U'\{Q(z-1)\}]$$
$$+ \alpha(z) V Q'(z), \tag{10}$$

for all $z \in [0, N]$. Periodic boundary conditions require that $Q(0) = Q(N)$, and the condition $\sum_{i=1}^{N} Q_i(t) \equiv 0$, implies that $\int_0^N Q(z) dz \equiv 0$.

If $f_e = 0$, the system simplifies to a 1D Hamiltonian lattice, and its corresponding differential-difference equation (10) may be solved analytically, at least for some nearest-neighbor interaction potentials, such as the Toda potential [9]. However, in the case $f_e \neq 0$ and $\alpha(z) \neq 0$, it does not seem possible to find an exact analytical solution for Eq. (10). Here we use a numerical approach. We discretize Eq. (10) by a finite difference method, and solve the resulting nonlinear equations by Newton's iteration method starting with an approximate solitary wave solution for the corresponding Hamiltonian system [9,10]. In this paper we focus on the well-known Fermi, Pasta, and Ulam β model that represents a 1D nonlinear lattice of widespread interest [11–13]. The interparticle interaction potential is $U(Q) = \frac{1}{2} Q^2 + \frac{1}{4} \beta Q^4$, $\beta = 1$. The soliton's configuration and its velocity-amplitude relationship for various values of f_e are obtained from Eq. (10).

In order to check that the solitons are indeed solutions of Eq. (1), direct numerical simulations of Eq. (1) are carried out with the solitons configuration being the initial conditions for (p_i, q_i). We find that the solitons are very stable
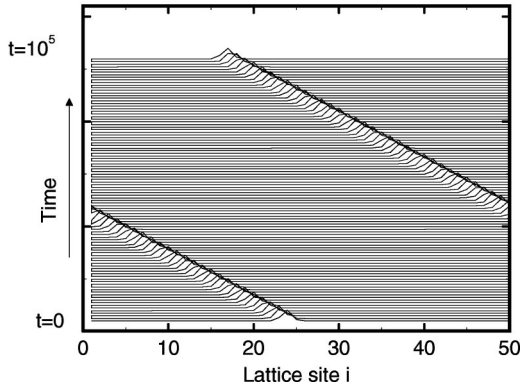
FIG. 1. The evolution of $Q_i(t) = q_{i+1}(t) - q_i(t)$ showing the propagation of a soliton with a constant velocity $V_s \approx 1.8$ in system (1) when the initial conditions are taken as the traveling wave solution of the differential-difference equation (10). The snapshot is taken every $\Delta t = 1000$ time units, during which the soliton has traveled about 1800 lattice sites (to the right), or 36 rounds in the periodic lattice. Here the field strength is $f_e = 0.003$. All units are dimensionless for the quantities plotted in this and other figures.

and travel in the system with a *preserved shape and velocity* for any field strength $0 \leqslant f_e \leqslant 0.01$. An example of such a soliton is shown in Fig. 1. Furthermore, by initializing more than one soliton in the initial conditions, we observe that the system supports multiple solitons of equal velocity. (If their velocities are different, the faster solitons will catch up to the slower ones and consume them during interactions.) Thus single and multiple solitons of equal velocity are steady states of this system.

Simulation results

However, if the system starts from *random* initial conditions what kind of steady state will it eventually reach? To answer this question, we have carried out extensive numerical simulations. Equations (1) are integrated using a fourth-order operator-splitting integrator [14] with a time-step size $\delta t = 0.002$. Periodic boundary conditions, i.e., $q_{N+1} = q_1$, $p_{N+1} = p_1$, are used. Unless indicated otherwise, the initial conditions for q_i and p_i are always prepared in the following way: initial values for q_i and p_i are randomly assigned and then rescaled to fix the system's energy to its given initial value, with the total momentum and the center of mass of the system being zero (thus they can remain so in the subsequent simulation). Then, a 10^6 time-step equilibrium simulation (Hamiltonian case $f_e = 0$) is made to reach a phase point [15], from which the nonequilibrium simulation of Eq. (1) for a nonzero external field strength is generated for a further 5×10^7 steps (i.e., 10^5 time units).

One of the most striking features to note is that for a given particle number N, and internal energy per particle, $E_p = \mathcal{H}/N$, the system dynamics behavior depends both on the initial conditions and the field strength f_e, and can be classified into two distinct types: spontaneous formation of a stable soliton, or chaotic dynamics throughout the simulation (see Fig. 2). Moreover, we have observed that in every case once a soliton is generated it never disappears but travels in
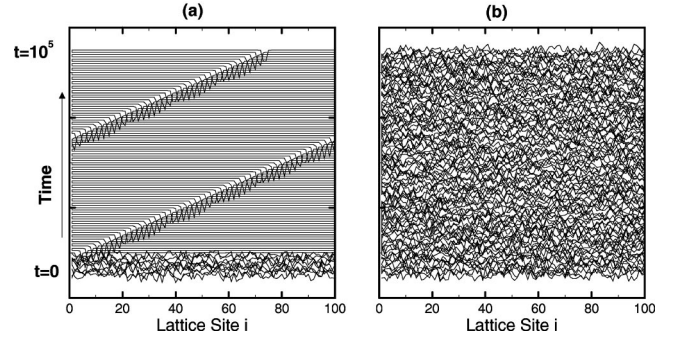

FIG. 2. The evolution of $Q_i(t) = q_{i+1}(t) - q_i(t)$ showing two types of steady state for system (1) with different random initial conditions: (a) spontaneous and irreversible formation of a soliton with a constant velocity $V_s \approx 2.9$, and (b) chaos throughout the simulation. Here $f_e = 0.0045$, and $E_p = 1.0$. Due to the symmetry of the equations of motion a soliton's maximum amplitude in Q_i can be either positive or negative.

the system for the entire length of the simulation run. This means that the transition from a chaotic to a soliton state is an irreversible process despite the equations of motion (1) being time reversible. We have verified that, unlike the situation for chaotic dynamics, the largest Lyapunov exponent for the soliton states is zero within statistical uncertainties. Therefore, the solitons are dynamically stable periodic orbits of this nonequilibrium system.

For a given field strength, there is a certain set of trajectories from which a soliton can emerge spontaneously. The probability of finding a soliton trajectory, denoted as P_S, is plotted in Fig. 3 as a function of the field strength. Here each data point is calculated from 20 sample trajectories that started from different random initial conditions. We observe that when f_e is smaller than a certain critical value $f_{C1} \approx 0.0040$, there is no spontaneous formation of solitons starting from the random initial conditions, thus the observed probability P_S is zero by definition (This does not mean that the soliton is not a solution of the system. In fact, a soliton can be observed if started from the right initial conditions—
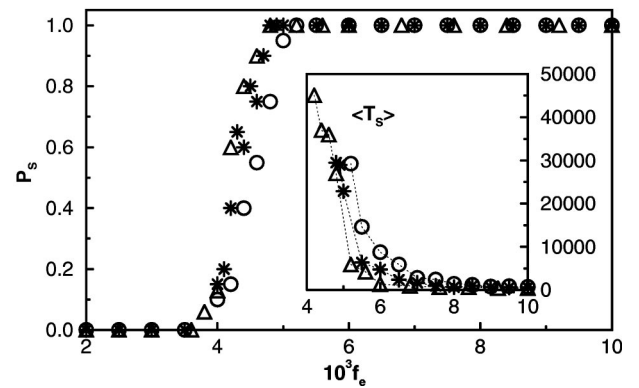

FIG. 3. The probability P_S and the average transient time $\langle T_S \rangle$ for soliton formation, as a function of the applied field strength f_e. The circles, stars, and triangles are for systems of 50, 100, and 200 particles, respectively. This figure shows qualitatively that there are multiple steady states in the system.

see previous discussion.) When f_e is greater than another critical value $f_{C2} \approx 0.0047$ the P_S becomes unity. A sharp transition is seen in P_S over the critical region (f_{C1}, f_{C2}) of the field strength. We find that while this behavior is qualitatively the same for different system size N, the chaos-soliton transition becomes sharper as the system size is increased.

Note that the values for P_S are estimated based on 20 sample trajectories and for a *given* very long but finite simulation time of 10^5 (these limits are imposed by finite computer resources). We believe that increasing the time length and the number of sample trajectories will not change the results of Fig. 3 qualitatively. The values for P_S would be increased a little bit for *every* field strength f_e smaller than $f_{C2} \approx 0.0047$, and the kinked curve for P_S will be slightly shifted towards the left if the simulation time is increased.

The transient time to generate a soliton from the random initial conditions, denoted as T_S, depends strongly on both initial conditions and the field strength. But the ensemble average $\langle T_S \rangle$ is nearly constant for large fields and yet it increases sharply when the field strength approaches the critical value f_{C1} from the large field region (see Fig.3). This behavior suggests that it is very computer time-consuming to determine accurately the critical field strength, f_{C1}, below which the probability of soliton generation is zero. For f_e in the critical region $(0.004 < f_e < 0.0047)$ the transient times for soliton formation vary widely between 0 to 10^5, giving an average value $\langle T_S \rangle$ much smaller than the upper limit (10^5) as shown in the inset of Fig. 3.

The dynamics of this system can be summarized as follows. For $f_e = 0$, the unforced Hamiltonian (conservative) system is nonergodic because it is chaotic for almost all random initial conditions, but periodic (solitons) for certain special initial conditions that form a set of *zero measure* (see also Refs. [11–13]). For $f_e > 0$ the system is dissipative and its comoving phase space shrinks (in dimension) as time goes on. In particular, some phase points collapse onto a low-dimension strange chaotic attractor, but others, which are sufficiently close to the soliton solution of the corre-

sponding Hamiltonian system, will be attracted onto the soliton solution of the dissipative system. The basin of attraction for the soliton grows as f_e increases, and eventually occupies the whole phase space when f_e crosses over a critical value.

The present multiple steady state phenomenon is different from the chaos-soliton transition phenomenon observed previously for NEMD 2D fluid particle systems and for 1D lattices of heat conduction with constant-temperature thermostat [6,8]. The latter systems were shown to be chaotic for small f_e and solitonic for large f_e, but their steady state appeared to be unique for a *fixed* heat field strength no matter what the initial conditions are. Furthermore, in the present paper, the multiple steady states exist for a fixed arbitrarily small field parameter, where both linear and nonlinear responses can be observed. This behavior is in contrast to the instability induced multiple steady states in hydrodynamics. In the latter case, the system must contain a large number of particles (e.g., about 50 000 particles were used in Ref. [16]); and the field parameters must exceed certain large critical values where the system responses become entirely nonlinear. See Ref. [16] and references therein.

In conclusion, we have demonstrated that for a given heat field strength $f_e < f_{C2}$ (no matter how small f_e is) the nonequilibrium heat flow system can reach either a solitonlike steady state or a chaotic attractor, *depending on the initial conditions.* Further investigations are necessary in order to understand a number of related issues, including how the multiple steady state phenomenon is related to the divergence of heat conductivities in 1D lattices [8,17–20], how the nonequilibrium fluctuation theories [4,5] should be modified to take into account the possibilities of multiple steady state, and finally, how solitons may affect the heat conduction of quasi-one-dimensional needlelike crystals such as carbon nanotubes. See Refs. [21,22] for experimental measurement of the heat conductivity of some needlelike crystals.

---

[1] D.J. Evans and G.P. Morriss, *Statistical Mechanics of Nonequilibrium Liquids* (Academic, New York, 1990). See http://www.rsc.anu.edu.au/~evans/evansmorrissbook.htm for an updated version of the book.

[2] W.G. Hoover, *Computational Statistical Mechanics* (Elsevier Science, Amsterdam, 1991).

[3] J.R. Dorfman, *An Introduction to Chaos in Nonequilibrium Statistical Mechanics* (Cambridge University Press, Cambridge, 1999).

[4] D.J. Evans and D.J. Searles, Phys. Rev. E **50**, 1645 (1994); **52**, 5839 (1995); **53**, 7808 (1996).

[5] G. Gallavotti and E.G.D. Cohen, Phys. Rev. Lett. **74**, 2694 (1995); J. Stat. Phys. **80**, 931 (1995).

[6] D.J. Evans and H.J.M. Hanley, Mol. Phys. **68**, 97 (1989); D.P. Hansen and D.J. Evans, *ibid.* **81**, 767 (1994).

[7] A. Maeda and T. Munakata, Phys. Rev. E **52**, 234 (1995).

[8] F. Zhang, D.J. Isbister, and D.J. Evans, Phys. Rev. E **61**, 3541 (2000).

[9] M. Toda, *Theory of Nonlinear Lattices* (Springer-Verlag, Berlin, 1981).

[10] J.A.D. Wattis, J. Phys. A **26**, 1193 (1993).

[11] E. Fermi, J. Pasta, and S. Ulam, Report No. LA-1940, 1955 (unpublished), reprinted in E. Fermi, *Collected Papers* (University of Chicago Press, Chicago, 1965), Vol. II, p. 978; J. Ford, Phys. Rep. **213**, 271 (1992).

[12] P. Poggi, S. Ruffo, and H. Kantz, Phys. Rev. E **52**, 307 (1995).

[13] L. Casetti, M.C. Sola, M. Pettini, and E.G.D. Cohen, Phys. Rev. E **55**, 6566 (1997).

[14] F. Zhang, J. Chem. Phys. **106**, 6102 (1997).

[15] This procedure of sampling may yield a microcanonical ensemble *if* the system's trajectories are ergodic [4]. However, the FPU model is known to be nonergodic, thus our sampling

method is not strictly microcanonical.

[16] S.T. Cui and D.J. Evans, Mol. Simul. **9**, 179 (1992).

[17] S. Lepri, R. Livi, and A. Politi, Phys. Rev. Lett. **78**, 1896 (1997); Physica D **119**, 140 (1998).

[18] B. Hu, B. Li, and H. Zhao, Phys. Rev. E **57**, 2992 (1998).

[19] T. Hatano, Phys. Rev. E **59**, R1 (1999).

[20] T. Prosen and D.K. Campbell, Phys. Rev. Lett. **84**, 2857 (2000).

[21] J. Hone, M. Whitney, C. Piskoti, and A. Zettl, Phys. Rev. B **59**, R2514 (1999).

[22] B. M. Zawilski *et al.* (private communications).